Clumpy coexistence in phytoplankton: The role of functional similarity in community assembly

Caio Graco-Roza [1, 4]*, Angel M Segura [2], Carla Kruk [3], Patrícia Domingos [1], Janne Soininen [4], Marcelo Manzi Marinho[1]

[1] Laboratory of Phytoplankton of Ecology and Physiology, Department of Plant Biology, University of Rio de Janeiro State, Rua São Francisco Xavier 524—PHLC Sala 511a, 20550-900, Rio de Janeiro, Brazil. Telephone: +552123340822

[2] Modelización Estadística de Datos e Inteligencia Artificial (MEDIA) CURE-Rocha, Universidad de la República, Uruguay.

[3] Sección Limnología, IECA, Facultad de Ciencias, Universidad de la República, Uruguay.

[4] University of Helsinki, Department of Geosciences and Geography, PO Box 64, FI00014, Helsinki, Finland. *correspondence author: caiogracor@gmail.com

Abstract

Emergent neutrality (EN) suggests that species must be sufficiently similar or sufficiently different in their niches to avoid interspecific competition. Such a scenario results in a multimodal distribution of species abundance along the niche axis (*e.g.*, body size), namely clumps. From this perspective, species within clumps should behave in a quasi-neutral state, and their abundance will show stochastic fluctuations. Plankton is an excellent model system for developing and testing ecological theories, especially those related to size structure and species coexistence. We tested EN predictions using the phytoplankton community along the course of a tropical river considering (i) body size structure, (ii) functional clustering of species in terms of morphology-based functional groups (MBFG), and (iii) the functional similarity among species with respect to their functional traits. Considering body size as the main niche axis, two main clumps (clump I and II) were detected in different stretches of the river and remained conspicuous through time. The clump I comprised medium-sized species mainly from the MBFG IV, while the clump II included large-bodied species from the groups V and VI. Pairwise differences in species biovolume correlated with species functional redundancy when the whole species pool was considered, but not among species within the same clump. Within-clump functional distinctiveness was positively correlated with species biovolume considering both seasons, and also at the upper course. These results suggest that species within clumps behave in a quasi-neutral state, but even minor shifts in trait composition may affect their biovolume. In sum, our findings point that EN belongs to the plausible mechanisms explaining community assembly in river ecosystems.

Keywords: species coexistence; emergent neutrality; functional distinctiveness; functional redundancy

Introduction

Understanding the mechanisms promoting species coexistence and shaping community structure has been a long-standing goal in community ecology. The former idea that the number of coexisting species is limited by the number of growth-limiting resources or niche dimensions (Gause 1936, Hardin 1960), and its derivate idea, "*the paradox of the plankton"* (Hutchinson 1957), have been widely explained in terms of endogenous and exogenous spatio-temporal mechanisms (Roy and Chattopadhyay 2007). Trait-based approaches are useful to test this matter due to their potential to generalize patterns beyond species' identity, especially because traits influence the species' ability to acquire resources and persist through environmental changes (McGill et al. 2006, Díaz et al. 2013, 2016). Nonetheless, niche-based theory proposes that the environment filters community composition through species' ecological requirements, which can be perceived through species' traits. However, at small spatial scales, species interactions present a predominant role, as the environmental heterogeneity is expected to be small (Götzenberger et al. 2012). In contrast, the more recent neutral theory suggests that diversity results from random dispersal, speciation, and extinction rates with no role of niche differences in species coexistence (Hubbell 2001). This type of dynamics should then result in random distribution of functional traits along environmental gradients (Kraft et al. 2008, Cornwell and Ackerly 2009).

More recently, it was shown that community organization is driven by eco-evolutionary processes such as speciation and nutrient uptake kinetics resulting in groups comprising different species with similar ecological requirements(Gravel et al. 2006, Hubbell 2006, Scheffer and van Nes 2006). This finding led to the 'emergent neutrality hypothesis' (EN) (Holt 2006) that has been supported by observational studies, e.g., for phytoplankton from brackish waters (Segura et al. 2011), birds from the North of Mexico (Thibault et al. 2011),

and beetles at the global scale (Scheffer et al. 2015). EN suggests that species must be sufficiently similar, and thus, behave neutrally, or different enough in their niches to avoid competition. Such a scenario would result in species-rich aggregations or clumps along the niche axis (Scheffer and van Nes 2006, Vergnon et al. 2009, Fort et al. 2010). Modelling studies have shown that such predictions apply for both steady environmental conditions (Fort et al. 2010), and also fluctuating resource conditions (Sakavara et al. 2018). Empirical evidence about EN is still scarce, however (Scheffer et al. 2018).

The clumpy pattern arises from the species niche preferences, meaning that species within clumps occupy same niche and their abundances are distributed stochastically (Scheffer et al. 2018). However, within a clump, trait differences may be important to species performance in the niche space (McGill et al. 2006, Violle et al. 2007), and it is difficult to state whether species behave neutrally within clumps (i.e., when the strength of interspecific interactions equals the intraspecific interactions). Zooming in on the uniqueness of trait combinations of species, i.e. functional distinctiveness, within clumps may advance our comprehension of biotic interactions and move towards a measurable value of similarity at which species coexistence is driven stochastically. Functional distinctiveness reflects the non-shared functions among species within a given species pool (Violle et al. 2007), mirroring the concept of functional redundancy (Pavoine et al. 2017). However, although two functionally redundant species most likely show high similarity in trait combination, functional distinctiveness is not directly linked to redundancy, and such metrics are often (Coux et al. 2016, Ricotta et al. 2016, Violle et al. 2017). For example, two species could show similar functional distinctiveness, i.e. the degree at which a species differs from all the others within the species pool concerning their functional traits, and still not be similar in their trait composition at a pairwise level (Coux et al. 2016). This suggests that both functional redundancy and distinctiveness are good metrics to assess the role of trait combination in

community assembly. To this end, planktonic communities offer an excellenta highly interesting model for biodiversity theory testing due to their highly speciose communities and their known relationship between morphological traits and function (Litchman and Klausmeier 2008, Kruk and Segura 2012, Litchman et al. 2012).

Body size is considered as a master ecological trait and it is highly useful to characterize species niche (Downing et al. 2014). In phytoplankton, the body size is related to physiology and life-history (Litchman and Klausmeier 2008), photosynthetic processes (Marañón 2008), nutrient uptake kinetics (Litchman et al. 2010)and other eco-evolutionary processes (Sauterey et al. 2017). Despite the importance of body size, the use of a single trait as a proxy for the niche may not evidence species differences generated by hidden niches and impair the understanding of clumpy patterns (D'Andrea et al. 2018). The use of multiple traits emerges as a powerful tool to disentangle plankton functional structure and evaluate competing hypotheses (Reynolds et al. 2014, Chen et al. 2015, Bortolini and Bueno 2017). Morphology-based functional groups (MBFG) classification of phytoplankton species (Kruk et al. 2010) uses a is a multidimensional combination of morphological traits that cluster organisms into seven groups with similar physiology and ecological responses (Kruk et al. 2011), potentially overcoming the limitations of using a single trait dimension only. Assessing the uniqueness in trait combinations of species within the same functional cluster (e.g., clumps, MBFGs) could help to study the existence of functional equivalence (i.e., neutrality) among species. Overall, the functional distance among species is a useful tool to compare species in a multidimensional space by comparing species' functional differences, particularly because the environment may filter different functional traits across space and time (Mouillot et al. 2013, D'Andrea et al. 2020).

Riverine ecosystems are highly heterogeneous andsystems characterized by a continuous water flow that affects the morphology, sedimentation patterns, dispersal, and phytoplankton diversity (Reynolds and Descy 1996, Wetzel 2001). Several theories explain the longitudinal occurrence and abundance of river phytoplankton communities, such as River Continuum (Vannote et al. 1980) and Flood Pulse (Junk et al. 1989) concepts. However, an explicit study of community size structure and phytoplankton species coexistence under EN in riverine ecosystems is lacking. For example, phytoplankton species should attain higher biomass at the middle reaches or in the upper reaches of low-gradient stretches, and the continuous water flow reduces the likelihood of biotic interactions (Reynolds et al. 1994). However, the physiological and morphological characteristics of species within the local species pool may result from eco-evolutionary processes that cluster species into limited functional groups that are favored under specific environmental conditions (Scheffer et al. 2015). Here, we push forward three hypotheses to be tested in a tropical river by investigating phytoplankton community size structure both seasonally and spatially:

H_1 – There are peak aggregations of species abundance (i.e., clumps) along the body size axis of phytoplankton in the river that remain constant across space and time as a result of eco-evolutionary processes.

H_2 – Differences in species biovolume scales positively with functional redundancy at the community-level but not at the clump level, because species within the same clump behave in a quasi-neutral state. Hence, the dominance within clump varies stochastically between redundant species because fitness differences would be negligible within clumps.

H_3 – There is a positive relationship between species abundance and species functional distinctiveness within clumps. Though abundance fluctuates stochastically at pairwise level, the number of species holding similar trait combinations may affect the likelihood of the

interactions within clumps. Therefore, species with the most distinct trait combinations with respect to their clump peers are less likely to share same ecological requirements, and by consequence, attain higher abundance.

Methods

Study area

Samples were taken monthly at nine stations along the Piabanha river between May 2012 and April 2013. Piabanha river is in the tropical region of Brazil and has a drainage basin of approximately 4500 km² (Figure 1). The headwater is on Petrópolis at 1546m altitude and drains to the medium valley of Paraíba do Sul river crossing three cities and with agricultural activities in their watershed. We set three river stretches (lower, medium and upper courses) based on the location of steep slopes the river elevation profile (Figure 1). Data from two meteorological stations, located close to the sampling sites, were used to measure rainfall. We analyzed meteorological data up to three days before each sampling campaign. We classified seasons as dry season (May - October) and a wet season (November – April) based on the rainfall data.

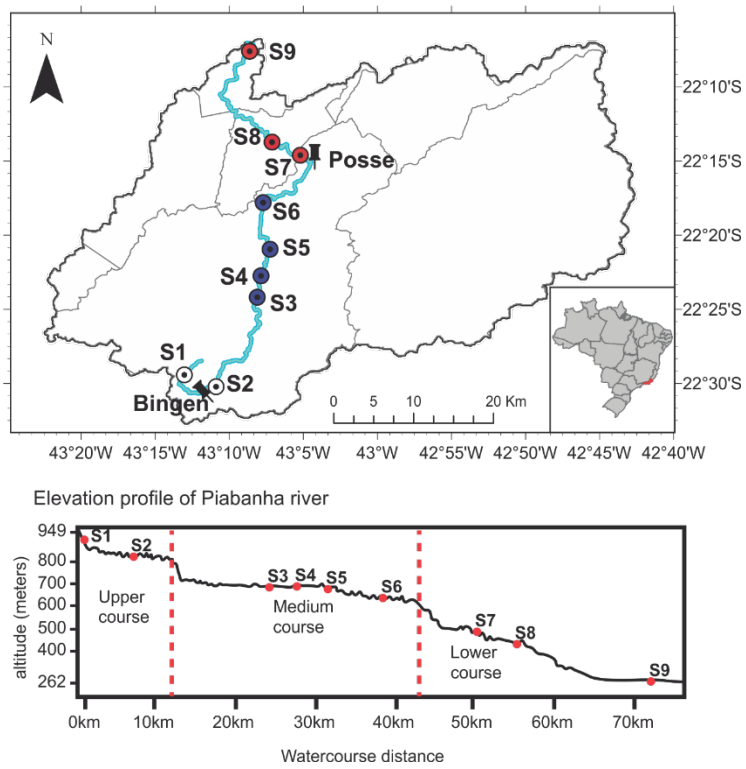

Figure 1. Map of the study area. The watershed area of the Piabanha river showing the river course (blue line) and the sampling sites colored according to river stretches (white circles = upper course, blue circles = medium course, red circles = lower course). The vertical dotted red line in the elevational profile figure indicates the locations of steep slopes used to define the boundaries of the river stretches.

Sampling and sample analysis

In the field, we measured temperature (°C), dissolved oxygen (DO, mg L^{-1}) and turbidity by a multiparameter probe sonde (YSI model 600 QS). Water discharge (WD, m^3 s^{-1}) was measured with the SonTek RiverSurveyor – M9. Furthermore, water samples were taken and kept frozen (one or 2 weeks) until the laboratory analysis for ammonium ($N{\cdot}NH_4^+$,mg L^{-1}), nitrate ($N{\cdot}NO_3^-$,mgL^{-1}), total phosphorus (TP, mg L^{-1}) and soluble reactive phosphorus (SRP, mg L^{-1}). The water samples were filtered (except for total phosphorus analysis) using borosilicate filters (Whatman GF/C), and nutrient concentrations were measured following

(APHA 2005). A complete description of the spatial and temporal patterns of the environmental variables measured in the Piabanha river can be found elsewhere (Graco-Roza et al. 2020).

Phytoplankton samples

Subsurface samples of phytoplankton were collected with a bottle of 200 mL and fixed with Lugol. In the laboratory, phytoplankton species were identified, and population densities estimated under an inverted microscope (Olympus CKX41) (Utermöhl 1958). At least 100 individuals of the dominant species were counted in each sample (error < 20%, $p < 0.05$, (Lund et al. 1958, Uhelingher 1964). Biovolumes ($mm^3\ L^{-1}$) were estimated by multiplying the density of each population by the average volume (V, μm^3), estimated from 20 random chosen individuals (whenever was possible), using the appropriate geometrical forms (Hillebrand et al. 1999, Sun and Liu 2003). In addition to the volume, we measured species' surface area (S, μm^2), the maximum linear dimension (MDL, µm), and the presence of aerotopes, mucilage, flagella, and siliceous exoskeleton. Hence, we used the volume and surface area of the species to estimate the individual surface volume ratio (SV). Species were then classified into Morphological Based Functional Groups (MBFG) according to (Kruk et al. 2010).

Traits-environment relationship

We tested the relationship between functional traits and the environmental variables using an RLQ analysis (Dolédec et al. 1996). The RLQ allows the visualization of the distribution of species traits and their related ecological preferences by testing the co-inertia between the matrices of environmental variables (R), species abundances (L), and species traits (Q). A Monte Carlo permutation test with 999 permutations at $\alpha = 0.05$ was used to test the statistical

192 significance of the RLQ axes. Furthermore, a fourth-corner method was applied to test the
193 statistical significance of all pairwise associations between species functional traits and
194 environmental variables. We quantified the strength of the associations using Pearson
195 correlation coefficient r_p, and the global statistics F-value (Legendre et al. 1997). The p-
196 values were corrected with 49999 permutations of the sites and the species to correct type I
197 errors, using false discovery rate method for adjusting p-values to control overall error rate
198 (Dray et al. 2014). However, because RLQ does not provide a significance test to identify
199 which combination of environmental variables acts on which combination of functional traits,
200 and the fourth-corner analysis tests the functional traits one at a time without considering the
201 covariation among traits and environmental variables, we used also a combined method of
202 RLQ and fourth-corner analysis (Dray et al. 2014). The significance of the associations was
203 tested by 99999 permutations of the sites and the species (Dray and Legendre 2008) to
204 correct type I errors, using false discovery rate method for adjusting p values to control the
205 overall error rate (Dray et al. 2014).

206 *Clumpy patterns*

207 To test for the existence of peak aggregations of species abundance along the body size axis
208 of phytoplankton - $\mathbf{H_1}$, we analyzed the community structure in each season (dry and wet) and
209 river stretches (upper, medium, and lower course). First, the individual volume of species was
210 log-transformed (log_2) and used as the main niche axis (X= log_2 volume). Hence, we divided
211 the niche axis into equally spaced segments (one segment per unit of log_2 biovolume) and for
212 each segment (j), we estimated the Shannon entropy (H) using the biovolume of the observed
213 species (Fort et al. 2010, Segura et al. 2011). The entropy index was defined as:

214 $$H_j = \sum_{i=1}^{n} p_i \, log_2(p_i), \quad (1)$$

215 where p_i is the fraction of biovolume of species *i* in the community of *n* species. Finally, we

tested the significance of the entropy (*H*) by comparing the observed *H* against an expected uniform distribution under the null hypothesis of homogeneous *H*. For this, we created 1000 communities by sampling the volume of species from a random uniform distribution bounded by observed individual volumes. Then, each species had a biovolume assigned to it, which was taken from a randomization of the observed biovolume matrix, keeping both the empirical species rank-abundance pattern and total biovolume in the sample. For each segment, the observed *H* was compared with the distributions of *H* generated under the null hypothesis, with significance defined according to standard 5% criterion (Fort et al. 2010; Segura et al. 2011).

Functional redundancy

To test whether differences in species biovolume scales positively with functional redundancy – $\mathbf{H_2}$, we first calculated the functional redundancy (F_{Red}) and the differences in biovolume between pairs of species using the whole community and using only the species from the clumps with significant entropy values. The functional redundancy was obtained by calculating Gower's general similarity coefficient [function *gowdis*, R package FD (Laliberté et al. 2014)] on the species functional traits. We used Gower's dissimilarity (*Gd*) because it can handle mixed variable types (continuous, binary, ordinal and categorical traits). *Gd* defines a distance value d_{jk} between two species as

$$d_{jk} = \frac{1}{N}\sum_{i=1}^{n}\left|\frac{(x_{ij}-x_{ik})}{max(x_i)-min(x_i)}\right|, \qquad (2)$$

where, *N* is the number of functional traits considered, x_{ij} the value of trait *i* for species *j* and x_{ik} the value of the trait *i* for species *k*. We thus tested $\mathbf{H_2}$ by conducting Mantel tests [function *mantel*, R package vegan (Oksanen 2017)] with 1000 randomizations, whenever

possible, on F_{Red} and $Diff_{Biov}$ matrices using all species, and separately for the species of each significant clump.

Functional distinctiveness (F_{Dist})

To test whether there is a positive relationship between species relative abundance at clump-level and species functional distinctiveness – **H_3**, we estimated the functional distinctiveness (F_{Dist}) as the distance of a species to the average trait position (centroid) in the multidimensional functional space for the set of species pertaining to each of the significant clumps using the equations proposed by Anderson (2006). First, we obtained species coordinates in the functional space by applying a Principal Coordinates Analysis (PCoA) in the species-by-traits data table using the Gower's dissimilarity (*Gd*). Hence, the distance from a species to its given centroid was calculated as

$$z_{ij}^{c} = \sqrt{\Delta^2\left(u_{ij}^{+}, c_{i'j'}^{+}\right) - \Delta^2\left(u_{ij}^{-}, c_{i'j'}^{-}\right)}, \qquad (3)$$

where Δ^2 is the squared Euclidean distance between u_{ij}, the principal coordinate for the *j*th point in the *i*th group, and c_i, the coordinate of the centroid for the *i*th group. The super-scripted '+' and '-' indicate the real and imaginary parts respectively (Equation 3, see Anderson 2006 for details). We did not weight the clump-centroid by species abundance and calculated F_{Dis} using all species pertaining to the significant clumps. Hence, to test **H_3**, we modeled the relationship between species biovolume and F_{Dist} using linear models. We used biovolume as response variable, with F_{Dist}, Clump position, and seasonal or spatial categories as fixed factors. Because the aggregation of sites across space and time have a nested design (i.e. spatial aggregation comprises all months sampled, and temporal aggregations comprises all sites sampled), we modelled spatial and temporal categories separately.

260 **Results**

261 Our samples included 150 species that were classified in six (MBFG I, III, IV, V, VI, and
262 VII) from the seven MBFGs based on their functional traits (Table 1). Species traits were
263 significantly associated with environmental variables (RLQ analysis; Figure 3; $P < 0.05$).
264 Individual volume (V), surface volume ratio (SV), maximum linear dimension (MLD), and
265 siliceous exoskeleton (Si) correlated significantly with the first axis, where SV had the
266 highest correlation ($r = -0.10$). Also, MLD and flagella correlated significantly with the
267 second axis ($r = - 0.07$, $r = -0.08$). For the environmental variables, water temperature (T) and
268 water discharge (WD) correlated the strongest with the first axis ($r = 0.10$ for both variables),
269 which also correlated significantly ($p< 0.05$) with total phosphorus (TP), dissolved oxygen
270 (DO), turbidity (Turb), and pH. In addition, dissolved inorganic nitrogen (DIN), soluble
271 reactive phosphorus (SRP), and turbidity (Turb) correlated significantly with the second axis,
272 and Turb had the highest correlation ($r= 0.90$) (Figure 2A).

Table 1. Distribution of species among the morphological-based functional groups.

MBFG	Number of species	Representative taxa
I	9	*Chroococcales* sp, *Chroococcus* sp.
III	3	*Limnothrix* sp.
IV	60	*Pseudoanabaena limnetica*, *Pseudoanabaena catenata*
V	13	*Euglena* sp. *Cryptomonas* sp.
VI	57	*Cymbella* sp., *Synedra* sp.
VII	8	*Dictyosphaerium* sp.
Total	150	

273 The distribution of the species belonging to different MBFGs in the RLQ ordination (Figure
274 2B) reflect their occurrence in relation to the environmental variables. The groups IV, V and
275 VI included 87% of the total number of species. Species from the group IV included
276 filamentous, colonial and unicellular species ranging from 21 μm^3 to 8181 μm^3 with no
277 specialized morphological traits (e.g. flagella, Si). Group V comprised unicellular flagellated

species ranging in size from 31µm³ to 31864 µm³, and group VI included unicellular and chain-forming species with siliceous exoskeletal body that ranged from 48µm³ to 19045µm³. According to the fourth-corner analysis, MLD was negatively correlated with pH (r = -0.09) and WD (r = -0.10), flagella was negatively correlated with Turb (r = -0.08), Si was positively correlated with Turb (r = 0.11) and WT (r = 0.09), whereas V was positively correlated with Turb (r = 0.08) (Figure 2C).

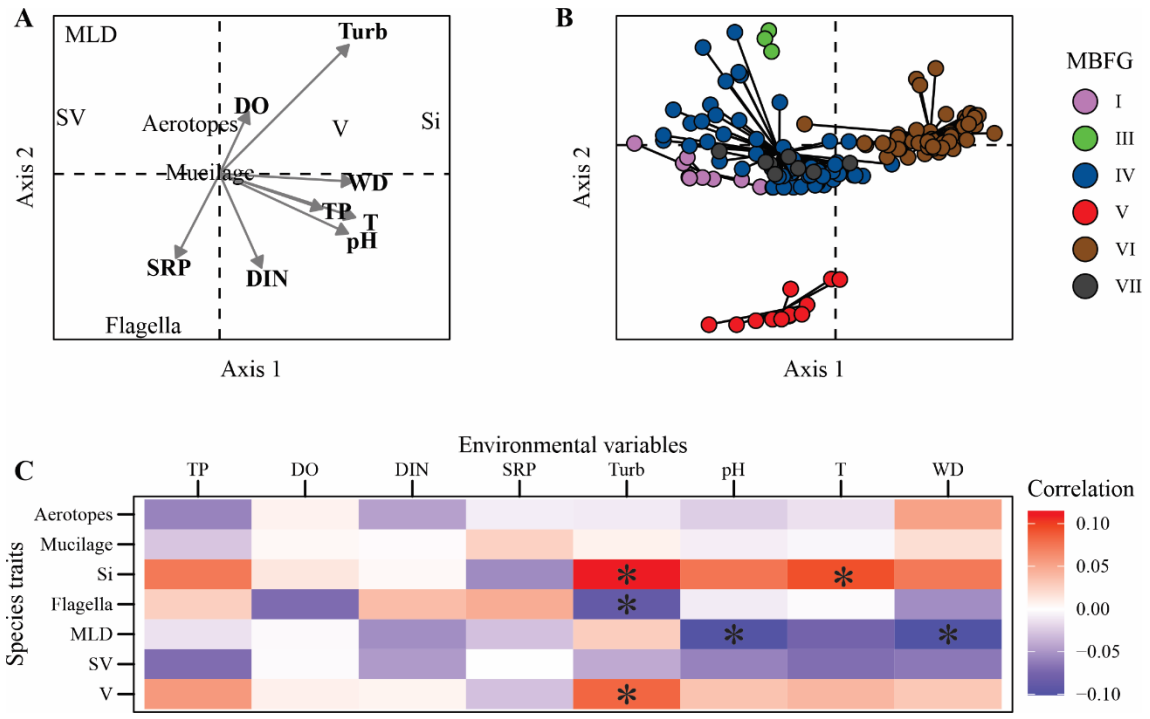

Figure 2. Results of the RLQ and fourth-corner analysis. (A) The relationships between species traits and environmental variables. First and second axes summarized 64.9% and 20.7% of variation, respectively. (B) The distribution of species in the functional space. Each point in the ordination plot within clusters represents the position of a species modelled according to its traits on RLQ axes 1 and 2. (C) The bivariate relationships between species traits and environmental variables. Functional traits are abbreviated as: Si = siliceous exoskeleton, MLD = maximum linear dimension, SV = surface volume ratio, V = individual volume. Environmental variables are abbreviated as: TP = total phosphorus, DO = dissolved

oxygen, DIN = dissolved inorganic nitrogen, SRP = soluble reactive phosphorus, Turb = turbidity, T = water temperature, WD = water Discharge.

The groups IV, V, and VI contributed to 95% of the mean biovolume of total phytoplankton in dry and wet seasons, and 96.6% across river stretches (Figure 3). The group VI had the highest contribution for the biovolume of almost all river stretches in both seasons, except for the upper course during dry season was dominated by the group IV (Figure 3). The entire list of species, functional traits, and assigned MBFG can be found in Table S1.

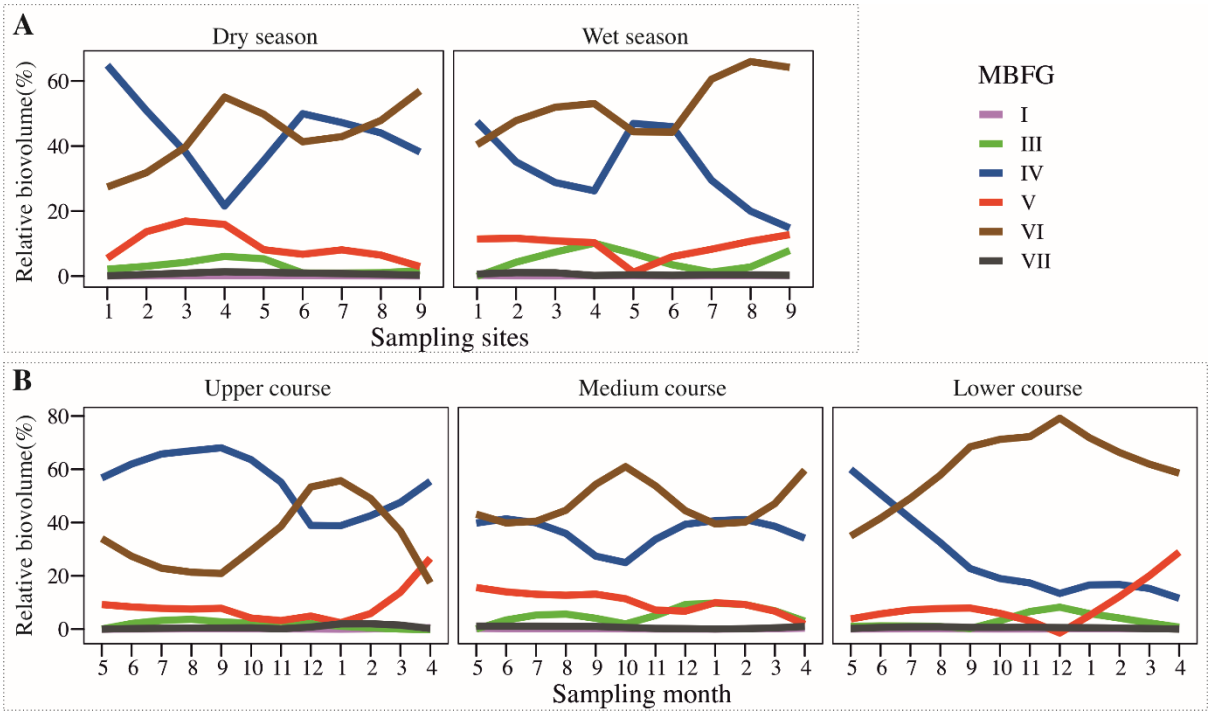

Figure 3. Relative contribution of morphology-based functional groups (MBFG) to total biovolume observed along the seasons and river stretches of the Piabanha river between May-2012 and April-2013. Trend lines are loess curves fit of each MBFG.

Overall, species individual volume ranged from 4.19 µm³ to 31864 µm³ totaling 14 equally spaced segments (S) of volume along the niche axis. From the 14 segments, three of them

showed significant entropy values, specifically S9, S13, and S14. This resulted in a biovolume aggregation (i.e. clumps) in two regions of the niche axis considering both temporal (Figure 4) or spatial categories (Figure 5). The first clump (Clump I) comprised species mainly from the group IV from S9 (e.g., *Pseudoanabaena limnetica*, *Pseudo anabaena catenata*), whereas the second clump (Clump II) included species from groups V and VI (e.g., *Euglena* sp., *Cymbella* sp.) at the segment S14. However, during the wet season, a few species from S13 also had significant entropy values and therefore were included in the clump II (Fig 4B).

The mean biovolume of species within clumps differed across seasons, but the identity of the most abundant species did not vary. *Pseudanabaena* sp. 4 (spp. 28) and *Pseudanabaena catenata* (spp. 12) had the highest biovolumes of clump I and held the highest biovolumes of the clump at both dry and wet seasons. Within the clump II, *Synedra* sp. (spp. 80) attained the highest biovolume during the dry season, whereas *Cymbella* sp. (spp. 051) contributed the most to clump biovolume in the wet season.

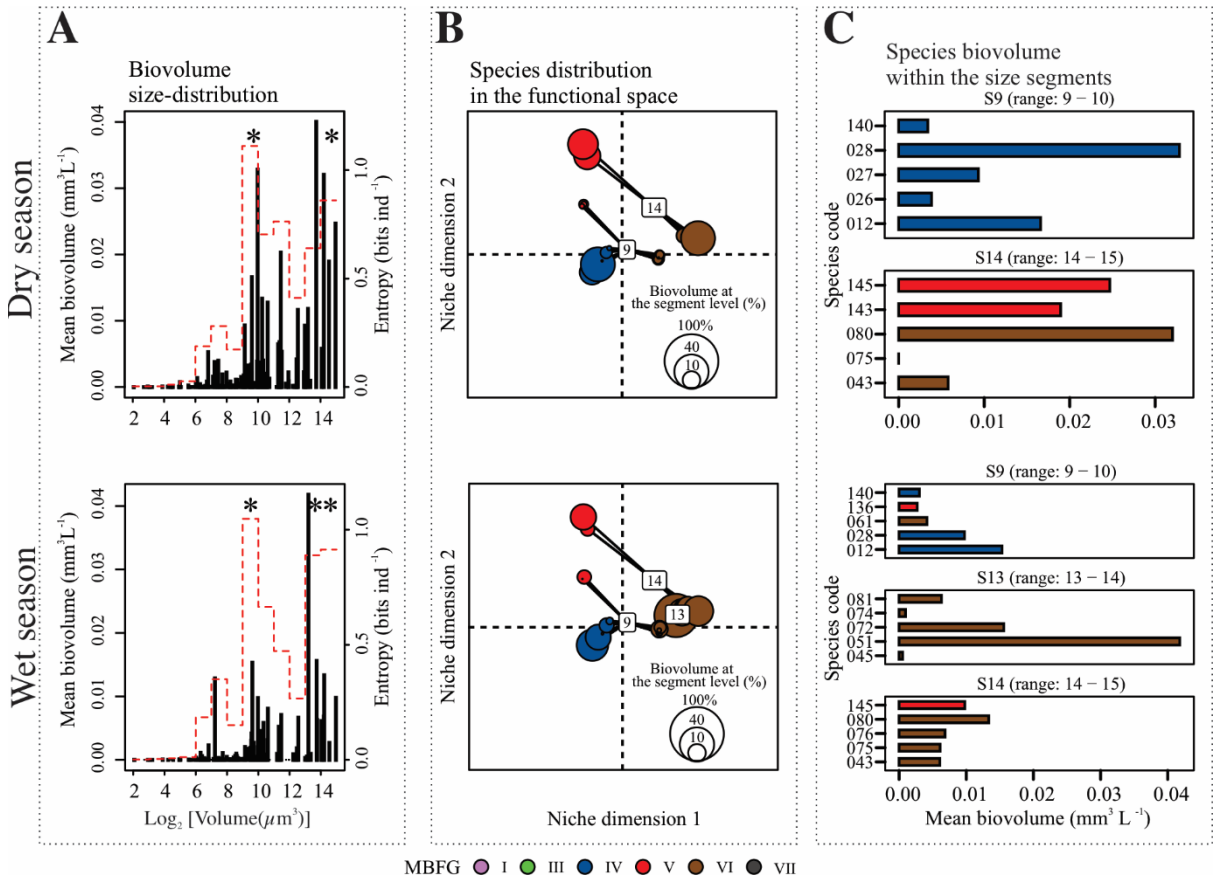

Figure 4. Distribution of phytoplankton biovolume along the body size axis, the ordination of species from the significant size segments (S) in the functional space, and the mean biovolume of the five most abundant species of each significant size segment during the dry and wet seasons of the Piabanha river, RJ. (A) Stem plots show size distribution in the sampling sites of the river Piabanha. Each stem represents a species with its body size (in $\log_2$) plotted on the abscissa and the mean biovolume plotted on the ordinate. The red dotted line indicates the entropy value of each size segment (i.e., one unit of $\log_2$ volume), and the asterisk highlights the significant entropy values tested through 1000 randomizations. (B) The species of the corresponding significant size-segment are ordinated in the functional space. The size of the circles represents the species contribution to the total biovolume of the size segment. (C) Bar plots (right show the biovolume of the five most abundant species from each significant size segment. Species are colored according to their morphology-based

functional groups (MBFG). The code of each species can be found in the supplementary material, Table S1.

Regarding the river stretches, *Pseudoanabaena* sp. 4 and *Pseudoanabaena catenata* contributed the most to the biovolume of the upper course, and only the clump I had significant entropy values for species from the S9 (Figure 5A). At the medium course, both the clump I and II had significant entropy values, mainly due to species from the S9 with *Pseudoanabaena* sp. 4 as the most abundant, and from the S14 with *Synedra* sp. as the most abundant (Figure 5B). At the lower course, the clump II had significant entropy values, specifically at the S14 where *Synedra* sp. contributed most to biovolume at segment level (Figure 5C).

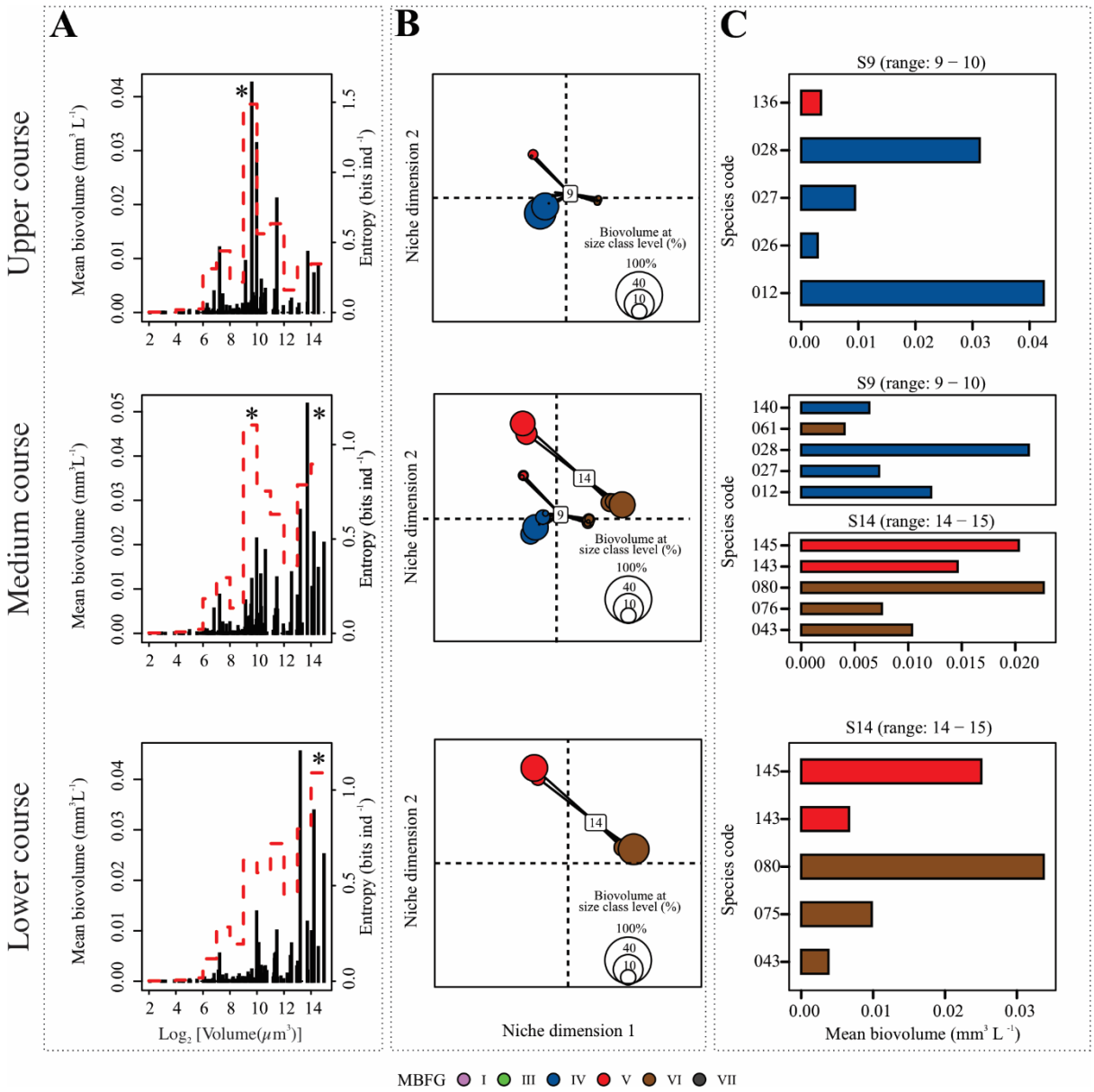

Figure 5. Distribution of phytoplankton biovolume along the body size axis, the ordination of species from the significant size segments (S) in the functional space, and the mean biovolume of the five most abundant species of each significant size segment at the upper, medium, and lower courses of the Piabanha river, RJ. (A) Stem plots show size distribution in the sampling sites of the river Piabanha. Each stem represents a species with its body size (in $\log_2$) plotted on the abscissa and the mean biovolume plotted on the ordinate. The red dotted line indicates the entropy value of each size segment (i.e., one unit of $\log_2$ volume), and the asterisk highlights the significant entropy values tested through 1000 randomizations.

348 (B) The species of the corresponding significant size-segment are ordinated in the functional
349 space. The size of the circles represents the species contribution to the total biovolume of the
350 size segment. (C) Bar plots (right show the biovolume of the five most abundant species from
351 each significant size segment. Species are colored according to their morphology-based
352 functional groups (MBFG). The code of each species can be found in the supplementary
353 material, Table S1.

354 Differences in biovolume among species were positively related to the functional redundancy
355 at the whole-community level, but not at the clump-level irrespectively to the season or river
356 stretch studied (Table 2). At the clump-level, we observed that species with higher
357 distinctiveness attained the highest biovolume in all the seasons and river stretches (except for
358 the lower course). The upscaling of biovolume with functional distinctiveness was observed
359 for species from both clumps, at different seasons and river stretches, but was particularly
360 different in the wet season, where species from clump II did not show any significant
361 relationship with biovolume, and at the medium and lower courses, where there were no
362 significant trends (Table 3).

363 **Table 2. Mantel correlation results.** Mantel correlation between the differences in species
364 biovolume and functional redundancy for the overall set of species and significant clumps
365 along the seasons (dry and wet) and river stretches (upper, medium and lower courses).

Seasons and river stretches	Stratum	Mantel correlation
Dry season		
	Overall	**0.180 (0.001)**
	Clump I	0.130 (0.120)
	Clump II	-0.172 (0.709)
Wet Season		
	Overall	**0.230 (0.001)**
	Clump I	0.065 (0.235)
	Clump II	-0.167 (0.705)
Upper course		

	Overall	**0.165 (0.002)**
	Clump I	0.065 (0.242)
Medium course		
	Overall	**0.171 (0.001)**
	Clump I	0.059 (0.217)
	Clump II	-0.168 (0.633)
Lower course		
	Overall	**0.258 (0.001)**
	Clump II	-0.167 (0.696)

Note: Significant ($p < 0.05$) values are in bold and p-values are inside parentheses

Table 3. Linear model results. Regression parameters of the relationship between species biovolume and functional distinctiveness at the clump level.

	Dependent variable: Log_{10} Biovolume				
	Biovolume				
	Dry season	Wet season	Upper course	Medium course	Lower course
F_{Dist}	14.925*	15.854*	24.440**	12.377	7.267
	(6.127)	(6.015)	(7.816)	(6.085)	(4.373)
Clump II	4.676	7.501*	9.619	4.373	2.067
	(6.148)	(3.175)	(18.074)	(5.169)	(3.689)
F_{Dist} × Clump II	-8.458	-15.863	-21.301	-7.911	-1.651
	(15.608)	(7.734)	(46.232)	(13.329)	(9.501)
Intercept	-8.979**	-9.748**	-12.951**	-7.945**	-6.165**
	(2.439)	(2.496)	(3.143)	(2.418)	(1.734)
Observations	26	31	19	28	26
R^2	0.420	0.437	0.457	0.374	0.579
Adjusted R^2	0.341	0.374	0.348	0.296	0.522
Residual Std. Error	0.756 (df = 22)	0.663 (df = 27)	0.823 (df = 15)	0.755 (df = 24)	0.523 (df = 22)
F Statistic	5.313**	6.987**	4.204*	4.778**	10.090**

	(df = 3; 22)	(df = 3; 27)	(df = 3;15)	(df = 3;24)	(df = 3; 22)

Note: $^{*}p < 0.05$ $^{**}p < 0.01$

Discussion

Present results showed that (i) the clumps in body size are a conspicuous feature of phytoplankton community structure in riverine systems across seasons and river stretches; (ii) species within clumps show random distribution of biovolume with respect to their pairwise functional differences, but functional redundancy is related to differences in biovolume at the whole-community level; and (iii) species biovolume generally scales positively with functional distinctiveness at the clump level. Note that, on the one hand, multimodal aggregation of species biovolume along body size axis only points to the integration of niche-based processes and neutrality driving community assembly (Vergnon et al. 2009), but it does not imply that EN is the only mechanism behind phytoplankton coexistence. On the other hand, our results do not support alternative hypothesisexplanations such as pure neutrality (Hubbell 2001) or high dimensional hypothesis (Clark et al. 2007) because pure neutrality predicts a uniform distribution of species biovolume along the niche axis (Hubbell 2001), and the HDH does not predict any particular trait distribution (Vergnon et al. 2009, Ingram et al. 2018).

One alternative theory that is likely to explain clumpy aggregations is the Holling's textural hypothesis (Holling 1992). The textural hypothesis explains multimodal species size distribution with environmental constraints, and although distribution of the clumps was spatially structured, our results do not support HDH as a whole. River stretches and seasons are radically different in river hydrology, nutrients and fluxes, but that was not reflected in phytoplankton size structure. Moreover, if landscape controls the body size pattern alone, differences in phylogenetics, biogeography, energeticsenergenitics, and community

interactions should not significantly affect such pattern (Allen et al. 2005). However, the clumps in our data were in the similar size range and comprised species from the same MBFG found in previous studies from different systems (Segura et al. 2011, 2013). More importantly, there was a clear functional differentiation of species between clumps in terms of MBFG (Figure 5-6), and the trait composition of the communities reflected adaptations to survive in different environmental templates (Kruk and Segura 2012). For example, species from the group IV dominated in low-flow waters with high nutrient input, while species from group V and VI show different adaptations to survive in turbulent and mixed conditions (Margalef 1978, Soares et al. 2007, Bortolini and Bueno 2017). Therefore, our findings corroborate our $\mathbf{H_1}$ on the existence of significant peak aggregations in species biovolume along the body size axis. Such results agree with previous evidence of EN using phytoplankton as the model community in coastal and estuarine environments (Segura et al. 2011, 2013), and shows that clumpy distributions are evident on the phytoplankton communities of riverine ecosystems presenting fluctuations in environmental conditions. In addition, our findings are in line with recent modeling results suggesting clumpy patterns arise in environments subjected to resources fluctuation (Sakavara et al. 2018). It remains to be tested the trade off between resources among competing species, which is the remaining ingredient for the emergence of clumps.

We expanded the level of analysis from mere size structure towards the inclusion of new trait dimensions by analyzing the functional similarity at MBFG classification level and functional redundancy. We found that the species from the same clump represent a selection of all the possibilities amongst MBGFs, reinforcing that body size is a good proxy for niche preferences of the species (Blanckenhorn 2000). However, assessing MBFGs helped to assign niche differences at a finer degree, taking into account that using only a single trait could impair the patterns behind community assembly (D'Andrea et al. 2018). Species within

the same MBFG are expected to share ecological strategy (Kruk et al. 2010, Kruk and Segura 2012) and accordingly to EN, would also perform similarly (Scheffer et al. 2018). Still, the importance of traits to equalize or stabilize niche differences are context-dependent and assessing the functional multidimensional space should help to unveil community assembly processes (Bonser 2006). Here, we found that size-related traits (volume, MLD) and the presence of flagella or siliceous exoskeleton were the main drivers of phytoplankton distribution. Not surprisingly, such traits are key determinants on the assignment of species to the main MBFG observed here (Kruk et al. 2010). Furthermore, we found that fitness differences were significant at the community level, but not at within-clumps level, even considering multiple morphological traits. Still, the dominance of medium-sized species (clump I) in the upper course and of large-bodied species (clump II) in the lower course suggests that the coexistence of these MBFGs tends to generate clumpy distributions that are eroded when the ecosystem properties favor the dominance of other MBFGs, but the fluctuations in biovolume within clumps remains stochastic even when clumps hold a few species belonging to different MBFGs. These findings corroborate our **H2** - differences in species biovolume scales positively with functional redundancy at the community level but not at within-clumps level - and reinforces the predictions on the quasi-neutrality state of species within clumps (Holt 2006).

We also outlined the role of functional similarity in community assembly by studying the effects functional distinctiveness on species biovolume at clump level. We found that at the clump I, species biovolume increased with functional distinctiveness, but this pattern was weaker within clump II. Despite the species from group V and VI show lower growth rates than the species from group IV (Kruk et al. 2010), their elongated shape provides advantage under turbulent conditions (Reynolds et al. 1994) favoring these species under high flow conditions on nutrient-rich environments (Irwin et al. 2006). Furthermore, nutrients are

hardly limiting phytoplankton growth especially in meso- or eutrophic rivers (Reynolds 2006), and large-bodied species are mostly randomly introduced from different habitats (e.g. periphyton or epiphyton) (Wang et al. 2014, Descy et al. 2017), which brings some uncertainty to the assumption of niche overlap due to size similarity. In fact, nutrients were not relevant for structuring the phytoplankton community of the Piabanha river, and we also observed a significantly different size-segment (S13) within the clump II during the high flow periods. Thus, one cannot be sure if species within clump II are truly occupying same niche or if they just were introduced to the plankton by random displacement. We suggest this may be the mechanism leading to the weak relationship between functional distinctiveness and biovolume within clump II.

Emergent neutrality results from eco-evolutionary processes that leads species selection towards a limited number of functional groups (Scheffer and van Nes 2006). This implies that the clumps observed here are not likely a result of competitive exclusion at the Piabanha river, but a convergent evolution of competing species over time as previously suggested (Macarthur and Levins 1967). Therefore, even when the competition rates are relaxed due to sufficient nutrient supply, some other limiting factors that are not consumed by biotic organisms such as heat energy or turbulence determine species biovolume, and even minor shifts in species trait combination may lead to higher biovolume with respect to other species occupying same niche. Our results showed that it is also possible to predict the biovolume of species within clumps, but only when neutral processes (e.g., species displacement) are relaxed and biotic interactions are more likely to occur. Therefore, our findings partially agree with $\mathbf{H_3}$ - there is a positive relationship between species abundance and species functional distinctiveness within clumps, but the environmental conditions seem to play a key role in the outcome.

In summary, we provided evidence of both neutral and niche perspective driving planktonic community assembly and support the view that emergent neutrality is a likely mechanism to explain species coexistence in an open and environmentally heterogeneous ecosystem. The use of MBFG classification and functional space to describe species within clumps revealed that under the same size range, species with a greater degree of redundancy alternate their dominance in an unpredictable way. The significance and dominance of the clumps were related to the environmental conditions, but the biovolume of species within the clumps was better predicted by functional distinctiveness than by pairwise functional redundancy. This addresses the difficulty to avoid the ghost of hidden niches (Barabás et al. 2013), and also provides evidence from multiple angles that points to EN as a plausible mechanism in shaping species coexistence.

Acknowledgments

CGR PhD scholarship was funded by Fudação de Apoio a Pesquisa do Estado do Rio de Janeiro (FAPERJ) and by Coordenação de Aperfeiçoamento de Pessoal de Nível Superior (CAPES). MMM was partially supported by CNPq (303572/2017-5).

References

Allen, C. R., L. Gunderson, and A. R. Johnson. 2005. The use of discontinuities and functional groups to assess relative resilience in complex systems. Ecosystems 8:958–966.

Anderson, M. J. 2006. Distance-based tests for homogeneity of multivariate dispersions. Biometrics 62:245–253.

APHA, A. 2005. WEF: Standard Methods for the Examination of Water and Wastewater: Centennial Edition. Washington, DC.

Barabás, G., R. D'Andrea, R. Rael, G. Meszéna, and A. Ostling. 2013. Emergent neutrality or hidden niches? Oikos.

Blanckenhorn, W. U. 2000. The Evolution of Body Size: What Keeps Organisms Small? The Quarterly Review of Biology 75:385–407.

Bonser, S. P. 2006. Form defining function: interpreting leaf functional variability in integrated plant phenotypes. Oikos.

Bortolini, J. C., and N. C. Bueno. 2017. Temporal dynamics of phytoplankton using the morphology-based functional approach in a subtropical river. Revista Brasileira de Botanica 40:741–748.

Chen, N., L. Liu, Y. Li, D. Qiao, Y. Li, Y. Zhang, and Y. Lv. 2015. Morphology-based classification of functional groups for potamoplankton. Journal of Limnology 74:559–571.

Clark, J. S., M. Dietze, S. Chakraborty, P. K. Agarwal, I. Ibanez, S. LaDeau, and M. Wolosin. 2007. Resolving the biodiversity paradox. Ecology Letters 10:647–659.

Cornwell, W. K., and D. D. Ackerly. 2009. Community assembly and shifts in plant trait distributions across an environmental gradient in coastal California. Ecological Monographs 79:109–126.

Coux, C., R. Rader, I. Bartomeus, and J. M. Tylianakis. 2016. Linking species functional roles to their network roles. Ecology letters 19:762–770.

D'Andrea, R., J. Guittar, J. P. O'Dwyer, H. Figueroa, S. J. Wright, R. Condit, and A. Ostling. 2020. Counting niches: Abundance-by-trait patterns reveal niche partitioning in a Neotropical forest. Ecology 101.

D'Andrea, R., A. Ostling, and J. P. O'Dwyer. 2018. Translucent windows: how uncertainty in competitive interactions impacts detection of community pattern. Ecology Letters 21:826–835.

Descy, J. P., F. Darchambeau, T. Lambert, M. P. Stoyneva-Gaertner, S. Bouillon, and A. v. Borges. 2017. Phytoplankton dynamics in the Congo River. Freshwater Biology 62:87–101.

Díaz, S., J. Kattge, J. H. C. Cornelissen, I. J. Wright, S. Lavorel, S. Dray, B. Reu, M. Kleyer, C. Wirth, I. Colin Prentice, E. Garnier, G. Bönisch, M. Westoby, H. Poorter, P. B. Reich, A. T. Moles, J. Dickie, A. N. Gillison, A. E. Zanne, J. Chave, S. Joseph Wright, S. N. Sheremet Ev, H. Jactel, C. Baraloto, B. Cerabolini, S. Pierce, B. Shipley, D. Kirkup, F. Casanoves, J. S. Joswig, A. Günther, V. Falczuk, N. Rüger, M. D. Mahecha, and L. D. Gorné. 2016. The global spectrum of plant form and function. Nature 529:167–171.

Díaz, S., A. Purvis, J. H. C. Cornelissen, G. M. Mace, M. J. Donoghue, R. M. Ewers, P. Jordano, and W. D. Pearse. 2013. Functional traits, the phylogeny of function, and ecosystem service vulnerability. Ecology and Evolution 3:2958–2975.

Dolédec, S., D. Chessel, C. J. F. ter Braak, and S. Champely. 1996. Matching species traits to environmental variables: A new three-table ordination method. Environmental and Ecological Statistics 3:143–166.

Downing, A. S., S. Hajdu, O. Hjerne, S. A. Otto, T. Blenckner, U. Larsson, and M. Winder. 2014. Zooming in on size distribution patterns underlying species coexistence in Baltic Sea phytoplankton. Ecology Letters 17:1219–1227.

Dray, S., P. Choler, S. Dolédec, P. R. Peres-Neto, W. Thuiller, S. Pavoine, and C. J. F. ter Braak. 2014. Combining the fourth-corner and the RLQ methods for assessing trait responses to environmental variation. Ecology 95:14–21.

Dray, S., and P. Legendre. 2008. Testing the species traits environment relationships: The fourth-corner problem revisited. Ecology 89:3400–3412.

Fort, H., M. Scheffer, and E. van Nes. 2010. The clumping transition in niche competition: A robust critical phenomenon. Journal of Statistical Mechanics: Theory and Experiment 2010.

Gause, G. F. 1936. The Struggle for Existence. Soil Science 41:159.

Götzenberger, L., F. de Bello, K. A. Bråthen, J. Davison, A. Dubuis, A. Guisan, J. Lepš, R. Lindborg, M. Moora, M. Pärtel, L. Pellissier, J. Pottier, P. Vittoz, K. Zobel, and M. Zobel. 2012. Ecological assembly rules in plant communities-approaches, patterns and prospects. Biological Reviews 87:111–127.

Graco-Roza, C., J. B. O. Santos, V. L. M. Huszar, P. Domingos, J. Soininen, and M. M. Marinho. 2020. Downstream transport processes modulate the effects of environmental heterogeneity on riverine phytoplankton. Science of the Total Environment 703.

Gravel, D., C. D. Canham, M. Beaudet, and C. Messier. 2006. Reconciling niche and neutrality: The continuum hypothesis. Ecology Letters.

Hardin, G. 1960. The Competitive Exclusion Principle.

Hillebrand, H., C.-D. D. Dürselen, D. Kirschtel, U. Pollingher, and T. Zohary. 1999. Biovolume calculation for pelagic and benthic microalgae. Journal of Phycology 35:403–424.

Holling, C. S. 1992. Cross-Scale Morphology, Geometry, and Dynamics of Ecosystems. Ecological Monographs 62:447–502.

Holt, R. D. 2006. Emergent neutrality. Trends in Ecology and Evolution 21:531–533.

Hubbell, S. P. 2001. The Unified Neutral Theory of Biodiversity and Biogeography. Page Monographs in Population Biology.

Hubbell, S. P. 2006. Neutral theory and the evolution of ecological equivalence.

Hutchinson, G. E. 1957. Concluding Remarks. Cold Spring Harbor Symposia on Quantitative Biology.

Ingram, T., R. Costa-Pereira, and M. S. Araújo. 2018. The dimensionality of individual niche variation. Ecology 99:536–549.

Irwin, A. J., Z. v. Finkel, O. M. E. Schofield, and P. G. Falkowski. 2006. Scaling-up from nutrient physiology to the size-structure of phytoplankton communities. Journal of Plankton Research.

Junk, W. J., P. B. Bayley, and R. E. Sparks. 1989. The flood pulse concept in river-floodplain systems. Canadian special publication of fisheries and aquatic sciences 106:110–127.

Kraft, N. J. B., R. Valencia, and D. D. Ackerly. 2008. Functional traits and niche-based tree community assembly in an Amazonian forest. Science 322:580–582.

Kruk, C., V. L. M. Huszar, E. T. H. M. Peeters, S. Bonilla, L. Costa, M. LüRling, C. S. Reynolds, and M. Scheffer. 2010. A morphological classification capturing functional variation in phytoplankton. Freshwater Biology 55:614–627.

Kruk, C., E. T. H. M. Peeters, E. H. van Nes, V. L. M. Huszar, L. S. Costa, and M. Scheffer. 2011. Phytoplankton community composition can be predicted best in terms of morphological groups. Limnology and Oceanography 56:110–118.

Kruk, C., and A. M. Segura. 2012. The habitat template of phytoplankton morphology-based functional groups. Hydrobiologia 698:191–202.

Laliberté, E., P. Legendre, B. Shipley, and M. E. Laliberté. 2014. Package 'FD.' Measuring functional diversity from multiple traits, and other tools for functional ecology.

Legendre, P., R. G. Galzin, and M. L. Harmelin-Vivien. 1997. Relating behavior to habitat: Solutions to the fourth-corner problem. Ecology 78:547–562.

Litchman, E., K. F. Edwards, C. A. Klausmeier, and M. K. Thomas. 2012. Phytoplankton niches, traits and eco-evolutionary responses to global environmental change. Marine Ecology Progress Series 470:235–248.

Litchman, E., and C. A. Klausmeier. 2008. Trait-Based Community Ecology of Phytoplankton. Annual Review of Ecology, Evolution, and Systematics 39:615–639.

Litchman, E., P. de Tezanos Pinto, C. A. Klausmeier, M. K. Thomas, and K. Yoshiyama. 2010. Linking traits to species diversity and community structure in phytoplankton. Hydrobiologia 653:15–28.

Lund, J. W. G., C. Kipling, and E. D. le Cren. 1958. The inverted microscope method of estimating algal numbers and the statistical basis of estimations by counting. Hydrobiologia 11:143–170.

Macarthur, R., and R. Levins. 1967. The Limiting Similarity, Convergence, and Divergence of Coexisting Species. The American Naturalist 101:377–385.

Marañón, E. 2008. Inter-specific scaling of phytoplankton production and cell size in the field. Journal of Plankton Research.

Margalef, R. 1978. Life-forms of phytoplankton as survival alternatives in an unstable environment. Oceanologica acta 134:493 509.

McGill, B. J., B. J. Enquist, E. Weiher, and M. Westoby. 2006. Rebuilding community ecology from functional traits. Trends in Ecology and Evolution 21:178–185.

Mouillot, D., N. A. J. Graham, S. Villéger, N. W. H. Mason, D. R. Bellwood, Mouillot, Graham, Villéger, Mason, Bellwood, D. Mouillot, N. A. J. Graham, S. Villéger, N. W. H. Mason, and D. R. Bellwood. 2013. A functional approach reveals community responses to disturbances. Trends in Ecology & Evolution 28:167–177.

Oksanen, J. 2017. Vegan: ecological diversity. R Package Version 2.4-4:11.

Pavoine, S., M. B. Bonsall, A. Dupaix, U. Jacob, and C. Ricotta. 2017. From phylogenetic to functional originality: Guide through indices and new developments. Ecological Indicators 82:196–205.

Reynolds, C., and J. Descy. 1996. The production biomass and structure of phytoplankton in large rivers. Arch. Hydrobiol. 113:161–187.

Reynolds, C. S. 2006. The Ecology of Phytoplankton. Page The Ecology of Phytoplankton. Cambridge University Press, Cambridge.

Reynolds, C. S., J. Alex Elliott, and M. A. Frassl. 2014. Predictive utility of trait-separated phytoplankton groups: A robust approach to modeling population dynamics. Journal of Great Lakes Research 40:143–150.

Reynolds, C. S., J. P. Descy, and J. Padisák. 1994. Are phytoplankton dynamics in rivers so different from those in shallow lakes? Hydrobiologia 289:1–7.

Ricotta, C., F. de Bello, M. Moretti, M. Caccianiga, B. E. L. Cerabolini, and S. Pavoine. 2016. Measuring the functional redundancy of biological communities: a quantitative guide. Methods in Ecology and Evolution 7:1386–1395.

Roy, S., and J. Chattopadhyay. 2007. Toxin-allelopathy among phytoplankton species prevents competitive exclusion. Journal of Biological Systems 15:73–93.

Sakavara, A., G. Tsirtsis, D. L. Roelke, R. Mancy, and S. Spatharis. 2018. Lumpy species coexistence arises robustly in fluctuating resource environments. Proceedings of the National Academy of Sciences of the United States of America 115:738–743.

Sauterey, B., B. Ward, J. Rault, C. Bowler, and D. Claessen. 2017. The implications of eco-evolutionary processes for the emergence of marine plankton community biogeography. The American Naturalist 190:116–130.

Scheffer, M., and E. H. van Nes. 2006. Self-organized similarity, the evolutionary emergence of groups of similar species. Proceedings of the National Academy of Sciences.

Scheffer, M., E. H. van Nes, and R. Vergnon. 2018. Toward a unifying theory of biodiversity. Proceedings of the National Academy of Sciences of the United States of America 115:639–641.

Scheffer, M., R. Vergnon, E. H. van Nes, J. G. M. Cuppen, E. T. H. M. Peeters, R. Leijs, and A. N. Nilsson. 2015. The Evolution of Functionally Redundant Species; Evidence from Beetles. PLOS ONE 10:e0137974.

Segura, A. M., D. Calliari, C. Kruk, D. Conde, S. Bonilla, and H. Fort. 2011. Emergent neutrality drives phytoplankton species coexistence. Proceedings of the Royal Society B: Biological Sciences 278:2355–2361.

Segura, A. M., C. Kruk, D. Calliari, F. García-Rodriguez, D. Conde, C. E. Widdicombe, and H. Fort. 2013. Competition drives clumpy species coexistence in estuarine phytoplankton. Scientific Reports 3:1–6.

Soares, M. C. S., V. L. M. Huszar, and F. Roland. 2007. Phytoplankton dynamics in two tropical rivers with different degrees of human impact (southeast Brazil). River Research and Applications 23:698–714.

Sun, J., and D. Liu. 2003. Geometric models for calculating cell biovolume and surface area for phytoplankton. Journal of Plankton Research 25:1331–1346.

Thibault, K. M., E. P. White, A. H. Hurlbert, and S. K. M. Ernest. 2011. Multimodality in the individual size distributions of bird communities. Global Ecology and Biogeography.

Uhelingher, V. 1964. Étude statistique dês méthodes de dénobrement planctonique. Archives des Sciences 77:121–123.

Utermöhl, H. 1958. Zur Vervollkommnung der quantitativen Phytoplankton-Methodik. SIL Communications, 1953-1996 9:1–38.

Vannote, R. L., G. W. Minshall, K. W. Cummins, J. R. Sedell, and C. E. Cushing. 1980. The River Continuum Concept. Canadian Journal of Fisheries and Aquatic Sciences 37:130–137.

Vergnon, R., N. K. Dulvy, and R. P. Freckleton. 2009. Niches versus neutrality: Uncovering the drivers of diversity in a species-rich community. Ecology Letters 12:1079–1090.

Violle, C., M.-L. Navas, D. Vile, E. Kazakou, C. Fortunel, I. Hummel, and E. Garnier. 2007. Let the concept of trait be functional! Oikos 116:882–892.

Violle, C., W. Thuiller, N. Mouquet, F. Munoz, N. J. B. Kraft, M. W. Cadotte, S. W. Livingstone, and D. Mouillot. 2017. Functional Rarity: The Ecology of Outliers. Trends in Ecology and Evolution 32:356–367.

Wang, C., X. Li, Z. Lai, Y. Li, A. Dauta, and S. Lek. 2014. Patterning and predicting phytoplankton assemblages in a large subtropical river. Fundamental and Applied Limnology / Archiv für Hydrobiologie 185:263–279.

Wetzel, R. G. 2001. Limnology: Lake and River Ecosystems. Third edition. Academic Press.